Two-phase flow pressure-drop type and thermal oscillations

M. M. Padki, H. T. Liu and S. Kakaç
Department of Mechanical Engineering, University of Miami, Coral Gables, FL, USA

This work focuses on the theoretical investigation of thermal and pressure-drop type instabilities in forced convection boiling in a vertical single channel system, with Freon-11 as the working fluid. Experiments with two nichrome tubes of 7.5 mm inner diameter and 9.5 mm outer diameter, one bare and one coated with Linde High-Flux coating, have been carried out. One series of experiments was conducted with constant fluid inlet temperature and various heat inputs, and another with constant heat input and varying inlet liquid temperature. Under the experimental conditions of the study, pressure-drop type and thermal oscillations, as well as pressure-drop type oscillations with superimposed density-wave oscillations, have been observed. A numerical model has been developed to predict the steady-state characteristics of the forced convective two-phase flow and the pressure-drop type and thermal oscillations in a boiling single channel. The drift-flux model is used for numerical predictions. Good agreement between the theory and experiments is obtained.

Keywords: two-phase flow instabilities; pressure-drop type oscillations; thermal oscillations; drift-flux model

Introduction

The phenomenon of thermal oscillations induced by two-phase flow is of importance for the design and operation of many industrial systems and equipment, such as steam generators, thermosyphon reboilers, refrigeration plants, and various heat exchangers used in chemical process units and refineries. The understanding of pressure-drop and density-wave type two-phase flow instability mechanisms is now essentially complete; some relevant work on the dynamic behavior of two-phase flow boiling systems concerning pressure drop and density-wave oscillations and the mathematical modeling of two-phase flows is cited.[1–20]

The experimental study, as well as analytical model, of thermal oscillations remains limited for two reasons. Firstly, the understanding of two-phase flow heat transfer in steady state is rather limited; secondly, the theoretical aspects of unsteady and oscillatory phenomena in convective heat transfer are not fully clarified yet. As the state-of-the-art on these fronts keeps developing, phenomena such as the one described in this work will be understood completely. Thus, the study of thermal oscillations is important for practical, as well as scientific, reasons.

In our experimental studies, thermal oscillations were observed, in addition to pressure-drop and density-wave oscillations. These are dynamic oscillations, accompanied by large fluctuations in the wall temperature. The flow oscillates between low quality (dryness fraction) and high quality regions at a given point in the heater. The wall superheat fluctuates correspondingly to accommodate the constant heat generation in the wall, as the heat transfer coefficient oscillates between wet and dry conditions. Kakaç et al.[10,11] presented experimental and theoretical investigations on thermal oscillations. The theoretical modeling was carried out under the assumption of homogeneous flow and thermodynamic equilibrium between the vapor and liquid phases. In this paper, some further work on the modeling of pressure-drop type and thermal oscillations is presented.

Experiments have been carried out with two nichrome tubes (7.5 mm inner diameter and 9.5 mm (outer diameter)—one bare and the other coated with Linde High-Flux coating—at various heat inputs (0, 400, 600, 800, and 1,000 W), keeping the inlet fluid temperature constant at room temperature. In another series of experiments, the heat inputs have been kept constant at 800 W, and the inlet liquid temperature varied between −10 and 23°C. Results obtained from the experimental work have been used to validate the modeling approach.

Address reprint requests to Prof. Kakaç at the Department of Mechanical Engineering, University of Miami Coral Gables, FL 33124, USA.

Received 8 June 1990; accepted 16 January 1991

Experimental investigations

Figure 1 is a schematic diagram of the two-phase flow loop, showing the basic dimensions and the instrumentation. The test-fluid, Freon-11, is supplied from the liquid container pressurized by nitrogen gas. A thermostatically controlled immersion heater in the liquid container and a cooling unit before the test section provide an inlet temperature range of −20 to 90°C, with a control accuracy of ±1.0°C. Following the 60.5-cm long electrically heated test section is a recovery section consisting of a condenser and a collector tank. The mixture of saturated liquid and vapor is led through the condenser coil, which is cooled by refrigerated brine at 0°C. The condensed liquid is then stored in a recovery tank that is maintained at a constant pressure to ensure constant levels of container and exit pressures.

All the tubing, except the recovery section, is made of 0.75 cm (0.295 in.) ID nichrome tube. In the recovery section, tubing of much larger diameter (1.90 cm ID) is used to minimize pressure losses. Two plenums of 6.35 cm (2.5 in.) ID are installed to simulate the inlet and exit headers of heat exchangers. The surge tank, which is an important dynamic component of

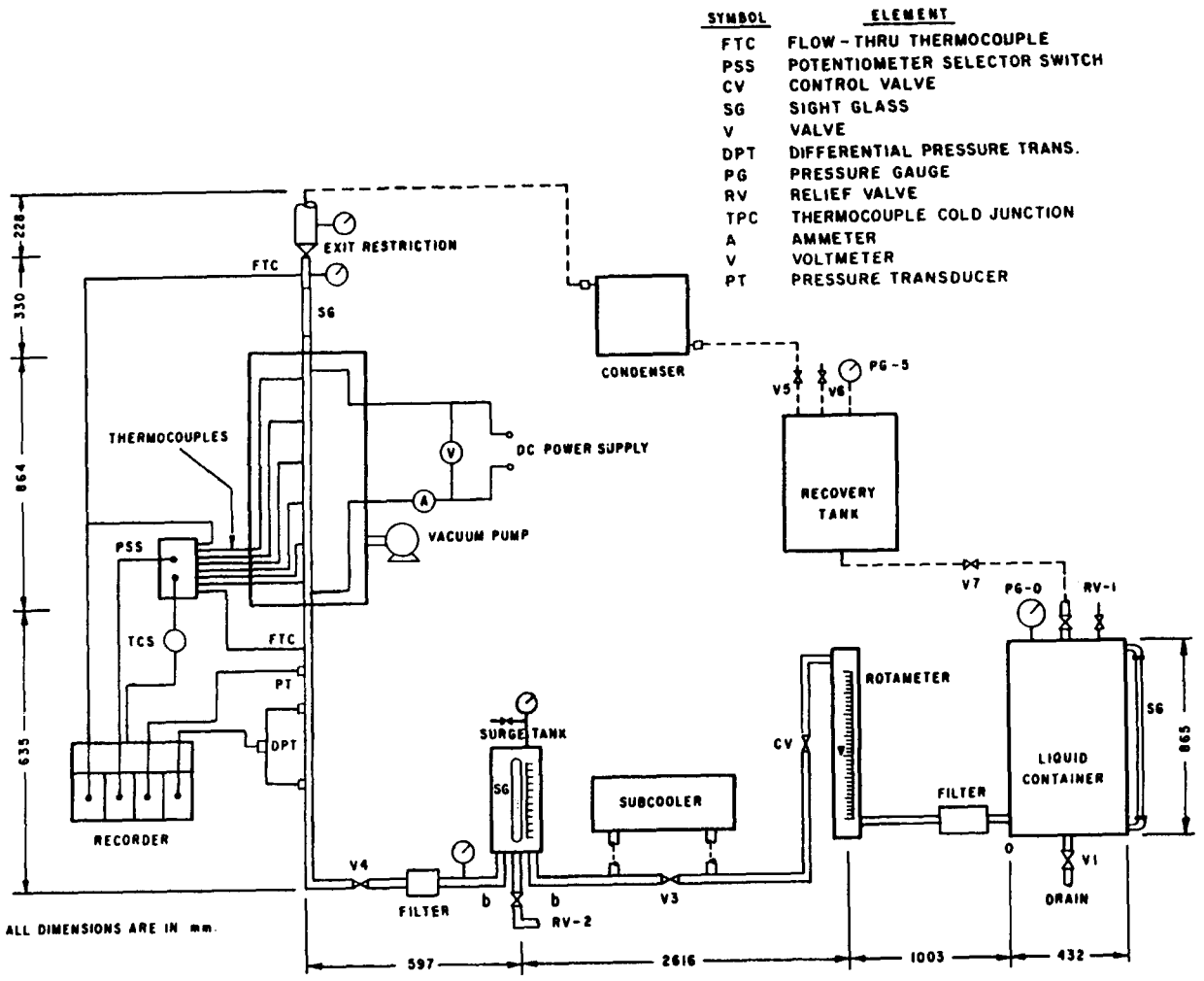

Figure 1 Schematic drawing of the experimental system

Notation

A_h Heater inner surface area, m^2
d Inner diameter of the heater tube, m
f Friction factor, dimensionless
F_m Two-phase flow friction multiplier, dimensionless
g Gravitational acceleration, 9.806 m^2/sec
G Fluid mass velocity ($=\rho u$), kg/(m^2 sec)
G_i Inlet mass velocity to surge tank, kg/(m^2 sec)
G_o Outlet mass velocity from surge tank, kg/(m^2 sec)
h Specific enthalpy of the fluid, J/kg
h_{lv} Latent heat of evaporation, J/kg
j Volumetric flux, m/sec
Nu Nusselt number, dimensionless
P Pressure, Pa
P_e Exit pressure, Pa
P_s Surge tank pressure, Pa
Q_I Heat input into the fluid, W
Q_o Rate of electric heat generation in the tube, W
t Time, sec
T_i Fluid inlet temperature, °C
u Fluid velocity, m/sec
x Quality of the liquid–vapor mixture, dimensionless
z Axial distance along the flow path, m

Greek symbols
μ Dynamic viscosity of the fluid, Pa s
ρ Density, kg/m^3
σ Surface tension, N/m
ϕ Heat input to fluid per unit volume of fluid, W/m^3
ψ Void fraction, dimensionless

Subscripts
e Exit
f Fluid
i Inlet
l Liquid
s Surge tank
v Vapor
w Wall

the loop, provides the necessary compressible volume for the pressure-drop oscillations to occur.

Appropriate instrumentation is installed to provide control and measurements of the test parameters, namely, flow rate, temperature, and pressure at various locations and the electrical heat input. Further discussion and details of the experimental set-up can be found elsewhere.[12]

Experimental procedure

For sustained instability experiments, the following experimental procedure has been developed.

For a given heater tube, different sets of experiments, corresponding to various heat inputs, have been conducted. For each heater tube, an initial experiment is conducted without any heat input, to determine the single-phase characteristics. Each set is composed of a sufficient number of tests to cover the available flow range. Stability boundaries have been determined in each case. Oscillations have been identified by the cyclic variations in pressures and flow rates, by observing the transparent section, the pressure-gauge pointers, and the recordings. In defining the stability boundary, short-life transients have been disregarded, and only sustained oscillations have been considered.

The procedure for the actual tests can be outlined as follows:

(1) With enough liquid in the liquid container tank, the tank is pressurized using nitrogen gas.
(2) The surge tank is half-filled with liquid Freon-11 and pressurized to a predetermined value by compressed air.
(3) The flow rate and the heat input are increased gradually to the desired starting point, and the system is allowed to become steady, as indicated by the recordings of system pressures, temperatures, and the flow rate.
(4) Measurements of temperatures, pressures, flow rate and heat input, and critical observations are noted.
(5) The mass flow rate is reduced by a small amount using the inlet control valve, and the system is allowed to become steady before the readings are noted down.

This procedure is repeated starting with step 4 until sustained oscillations are observed. After reaching the unstable region, the mass flow rate is first increased into the stable region and then decreased in small steps to precisely locate the instability boundary.

(6) While operating in the unstable region, firstly the heater inlet pressure and temperature are recorded. Then the system is stabilized by closing the inlet throttling valve slowly. After taking the readings, the inlet valve is brought into the fully open position, and the mass flow rate is further reduced by a small amount.

Following each adjustment, the system is allowed to stabilize, and the procedure is continued. The experiment is stopped after the dry-out point is reached.

Experimental results

Figure 2 shows some typical recordings of the oscillations obtained during the experiments, as reported.[12] The recordings of oscillations of heater inlet pressure, heater exit temperature, and mass flow rate are shown under the same operating conditions. It can be seen that both oscillate in phase with each other. The pressure oscillations can be seen to consist of two different kinds of oscillations: one, the main pressure-drop type oscillations, which have periods of the order of 20 to 60 sec, and two, the high-frequency density-wave type oscillations, which can be seen to be superimposed on the rising portions of the pressure-drop oscillations. The density-wave type oscillations have periods of the order of 2 to 7 sec.

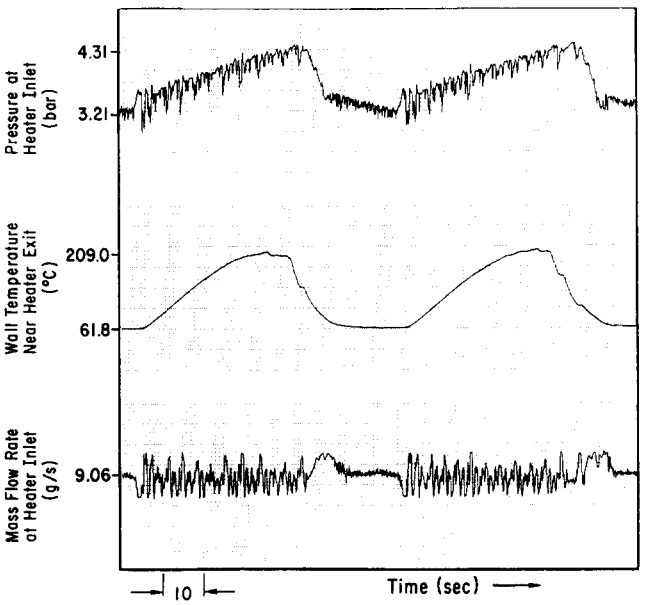

Figure 2 Typical superimposed oscillations. Heat input, 800 W, inlet fluid temperature, 10°C. Operating mass flow rate, 9.06 g/sec. Heater: coated nichrome, ID 7.5 mm, OD 9.5 mm

The phase relations among the three oscillating quantities can be seen to be as follows: When the mass flow rate is at the lowest point, the flow inside the heater is predominantly vapor with consequent low heat transfer coefficient, and the wall temperature is at its highest. In a similar way, the wall temperature is the lowest when the mass flow rate is high, since the predominantly liquid flow can carry away the heat better. When the heater inlet pressure drops, i.e., when the surge tank discharges the fluid it has stored in the previous cycle, the mass flow rate through the heater increases. Similarly, the mass flow rate through the heater decreases when the surge tank is charging and the heater inlet pressure is increasing.

Experimental uncertainties

Standard chromel-contantan thermocouple wires were used in the temperature measurements and a comparison calibration method was adopted in this study. The uncertainty for temperature measurement is about ± 0.5°C.

The inlet mass flow rate was measured by a rotameter in millimeters, and converted to grams per second by proper calibration. The calibration curve fitting polynomial was given elsewhere;[13] the overall uncertainty for mass flow rate is about ± 2 percent.

Heat input to the test section was calculated using the recorded voltage drop values over the heater tube and over the shunt circuit. With appropriate conversions, the reading of the voltage drop over the shunt circuit in millivolts was converted into the current value in Amperes. The heat input was then calculated as the product of these two. The total heat input to the test section was assumed to be equal to the electrical energy supplied to the heater tube without any loss. The overall uncertainty for heat input is about ± 2 percent.

Theoretical study

In the most general formulation of the two-phase flow problem, the conservation equations are written separately for each of

the phases. Various forms of the conservation equations have been proposed in the literature.[1–4] In order to reduce the complexity involved in the formulation of the problem in the most general case, several models have been suggested, which attempt at correlating different parameters of the two phases, such as drift velocity, void fraction, and slip ratio. In most of the practical problems, one-dimensional time-dependent equations are used. In this paper, the drift-flux formulation has been used, which has gained much acclaim in the last decade, taking into account the relative velocity between the phases, while assuming thermodynamic equilibrium between phases. This work, to the authors' knowledge, is the first application of the drift-flux model to the prediction of dynamic instabilities.

Mathematical formulation of drift-flux model

The equations that are used to describe the two-phase flow inside the constant area duct are one-dimensional transient equations for conservation of mass, momentum, and energy.

Conservation equations. The governing equations of two-phase flow are given by[2]:

(a) Continuity

$$\frac{\partial}{\partial t}[\rho_l(1-\psi)+\rho_v\psi]+\frac{\partial}{\partial z}[\rho_l u_l(1-\psi)+\rho_v u_v\psi]=0 \tag{1}$$

(b) Energy

$$\frac{\partial}{\partial t}[\rho_l h_l(1-\psi)+\rho_v h_v\psi]+\frac{\partial}{\partial z}[\rho_l u_l h_l(1-\psi)+\rho_v u_v h_v\psi]=\phi \tag{2}$$

(c) Momentum

$$-\frac{\partial p}{\partial z}=\frac{\partial}{\partial t}[\rho_l u_l(1-\psi)+\rho_v u_v\psi]+\left[\frac{\partial p}{\partial z}\right]_{\text{fric}}+\frac{\partial}{\partial z}\left\{G^2\left[\frac{(1-x)^2}{\rho_1(1-\psi)}+\frac{x^2}{\rho_v\psi}\right]\right\}+g[\rho_1(1-\psi)+\rho_v\psi] \tag{3}$$

where the subscripts l and v refer to liquid and vapor phases, respectively. The kinetic and potential energy terms have been neglected.

Auxiliary terms. The various auxiliary terms in the governing equations are defined below.

(d) Mass velocity, G,

$$G=\rho_l u_l(1-\psi)+\rho_v u_v\psi \tag{4}$$

(e) Quality (dryness fraction), x,

$$x=\frac{\rho_v u_v A_v}{\rho_l u_l A_l+\rho_v u_v A_v} \tag{5}$$

(f) Void fraction, ψ,

$$\psi=\frac{A_v}{A} \tag{6}$$

(g) Total enthalpy, h, at a given station,

$$h=\rho_l h_l(1-\psi)+\rho_v h_v\psi \tag{7}$$

Equations of state. These are supplied in the following form: for subcooled liquid, properties are calculated using the local temperature, while for saturated liquid and vapor, they are calculated using the local pressure.

Two-phase fraction coefficient. To get the $(\partial P/\partial z)_{\text{fric}}$ term in Equation 2, the frictional pressure-drop is expressed in terms of the local liquid-phase velocity, u_l, and the friction factor, f, calculated from an experimentally obtained correlation of Blasius-type.

The kinematic correlation. For the conservation equations to constitute a working model, i.e., to close the set of equations, the phase velocities, u_l and u_v, have to be related to the bulk flow rate and other flow parameters. The model to be used in the present study was originally proposed by Zuber and Findlay.[5]

A volumetric flux, which is the velocity of the center-of-volume of the fluid, is defined for the two-phase mixture as follows:

$$j=u_l(1-\psi)+u_v\psi \tag{8}$$

which can be written in terms of the mass velocity, G, as,

$$j=G\left[\frac{1-x}{\rho_l}+\frac{x}{\rho_v}\right] \tag{9}$$

According to the Zuber–Findlay model,[5] the vapor velocity, u_v, may be related to the volumetric flux as,

$$u_v=C_o j+u_{vj} \tag{10}$$

where C_o is a distribution parameter and u_{vj} is the drift velocity of the vapor phase with respect to the center of mass of the mixture. In the literature, there are various correlations for C_o and u_{vj}, depending primarily on the flow pattern. The following expressions used in the present study are reported to give good results for high-pressure steam-water flows irrespective of the flow pattern[4]:

$$C_o=1.13 \tag{11a}$$

$$u_{vj}=1.41\left[\frac{\sigma g(\rho_l-\rho_v)}{\rho_l^2}\right]^{1/4} \tag{11b}$$

It was confirmed that this set of correlations are not sufficient to predict the void fraction over the entire range of quality, and it was decided to adopt a two-regime model. Equations 11a and b were used till the quality was less than 0.2, and beyond that the correlations proposed by Ishii for annular flow were used.[4] These are

$$C_o=1.0 \tag{12a}$$

$$u_{vj}=23\left[\frac{\mu_l j_l}{\rho_v^D}\right]^{1/2}\frac{\Delta\rho}{\rho_l} \tag{12b}$$

Steady-state characteristics

The study of two-phase flow dynamic instabilities, in general, requires the knowledge of the steady-state pressure-drop versus mass flow rate characteristics, over the range of interest. The instability boundaries for pressure-drop type and density-wave type oscillations are usually shown on the plot of these relationships. These relationships, which are the steady-state solutions to the conservation equations, are also used to determine the initial conditions for both pressure-drop and density-wave type oscillations.

The single channel upward boiling flow apparatus has been simulated in this model as shown in Figure 3. Freon-11 enters the system from the liquid container at the point designated as I. The outlet of the surge tank is O. For ease of analysis and description, the flow path is divided into a number of regions, each with distinct flow characteristics. The part of the system from the surge tank to the inlet of the heater is called region 1. The subcooled part of the heater is called region 2, and the rest of the heater, where boiling takes place, is called region 3. Region 4 extends from exit of the heater to exit restriction. The exit restriction is treated separately as region 5, as described next.

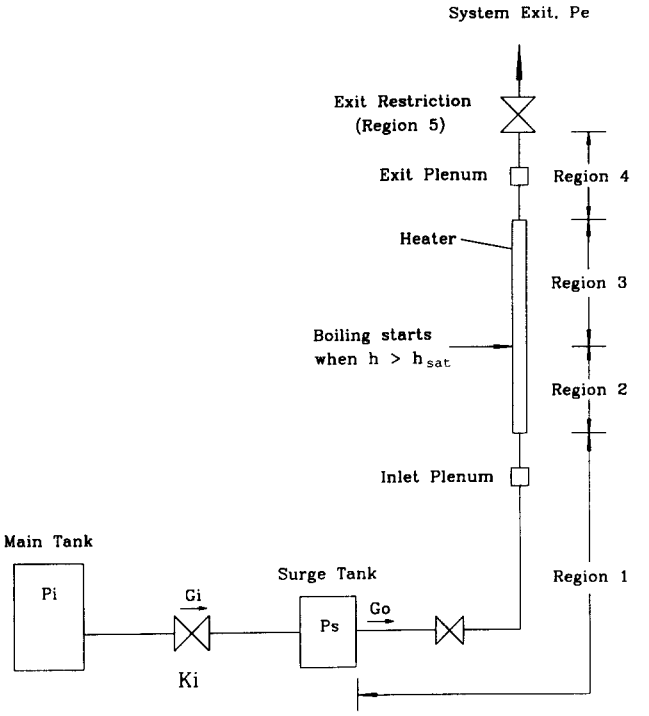

Figure 3 Schematic diagram of the model for finite-difference analysis

Exit restriction. The flow restriction at the system exit is a sharp-edged orifice with an orifice diameter of 1.59 mm. An empirical correlation, based on previous data, is used to calculate the pressure-drop across the restriction. The liquid-phase pressure-drop across the exit restriction is correlated as

$$\Delta P_e = 580(G^2/\rho_l) \tag{13}$$

where G is the mass velocity.

To correlate the two-phase pressure-drop data, a two-phase friction multiplier model is used. The two-phase friction multiplier F_m has been correlated as a function of the exit quality x_e as

$$F_m = 1 + 40x_e + 100x_e^2 - 50x_e^4 \tag{14}$$

Thus the two-phase pressure-drop across the exit restriction becomes .

$$\Delta P_e = F_m(580G^2/\rho_l) \tag{15}$$

Boundary conditions. The conservation equations, together with the equations of state and the constitutive relations, are to be solved for the following boundary conditions:

constant inlet temperature, T_i = constant

constant heat input, Q_I = constant

and, constant exit pressure, P_e = constant

Schema of solution. Calculations start with given values of mass velocity G, inlet fluid temperature T_i, heat input Q_I, and exit pressure P_e. Assuming an inlet (surge tank) pressure P_s, the flow parameters and properties are calculated from the exit of the surge tank to the inlet of the heater. The enthalpy, pressure, and density are calculated at each successive node in the heater. At each step, the enthalpy is checked against the saturated enthalpy at that pressure. Boiling is assumed to start when the fluid enthalpy exceeds the saturation enthalpy. Appropriate state and constitutive equations are chosen according to the state of the fluid. The calculation is continued along the rest of the system. The calculated exit pressure is checked against the given value P_e. If the difference is found to be within an acceptable margin, the assumed value of P_s is substituted for the surge tank pressure; otherwise the whole procedure is repeated with a different value of P_s, till convergence is obtained.

Time-dependent solutions

Taking the method and results developed in the previous sections, the time-dependent problem is tackled to predict pressure-drop type and thermal oscillations.

Model for pressure-drop oscillations. Pressure-drop oscillations occur in systems that have a compressible volume upstream of or within the heated section. They are usually confined to the middle portion of the negative slope region of the pressure-drop versus mass flow rate curve. The periods of typical pressure-drop oscillations are much larger than the residence time of any fluid particle in the flow; hence the pressure-drop oscillations are assumed to take place as a succession of quasisteady-state operating points of the system. The conditions provided by the steady-state solution are used as the initial conditions for the time-dependent solution.

The system under consideration is again as in Figure 3. The equations that describe the surge tank dynamics must be included in the analysis, since the air-vapor mixture inside the surge tank plays an important role in generating and maintaining the oscillations.

Governing equations

(a) Continuity equation for the surge tank[7]:

$$\frac{d(P_s)}{dt} = P_s^2 \frac{(G_i - G_o)A_p}{(P_{so}V_o\rho_l)} \tag{16}$$

where P_s is the surge tank pressure, P_{so} the steady pressure of the air in the surge tank, V_o the steady-state gas volume in the surge tank, G_i and G_o the inlet and outlet mass velocities to and from the surge tank, and ρ_l liquid density.

(b) Momentum equation for the mass velocity from main tank to surge tank

$$G_i = \left[\frac{(P_o - P_s)\rho_l}{R}\right]^{1/2} \tag{17}$$

where R is the restriction coefficient from the main tank to the surge tank, obtained from experimental data.

(c) The steady-state solution, which is assumed to be valid at every point of the pressure-drop oscillation, is obtained from the steady-state form of the governing equations. These relations, from the surge tank to system exit, can be written as

$$G_o = F(P_s, Q_I) \tag{18}$$

During the oscillations, the heat input Q_I and surge tank pressure P_s change, thus G_o becomes the dependent variable of Q_I and P_s.

Method of solution

An explicit forward difference technique is used to solve the nonlinear partial differential equations which describe the system dynamics. The governing equations (16, 17 and 18) are approximated by the method of forward finite differences.

The calculations start with given inlet fluid temperature and pressure. The initial flow parameters and properties, corresponding to the given inlet mass velocity and heat input, are calculated using the steady-state program. These results are saved as the initial conditions at the stable operating point.

The system is perturbed by increasing the pressure in the

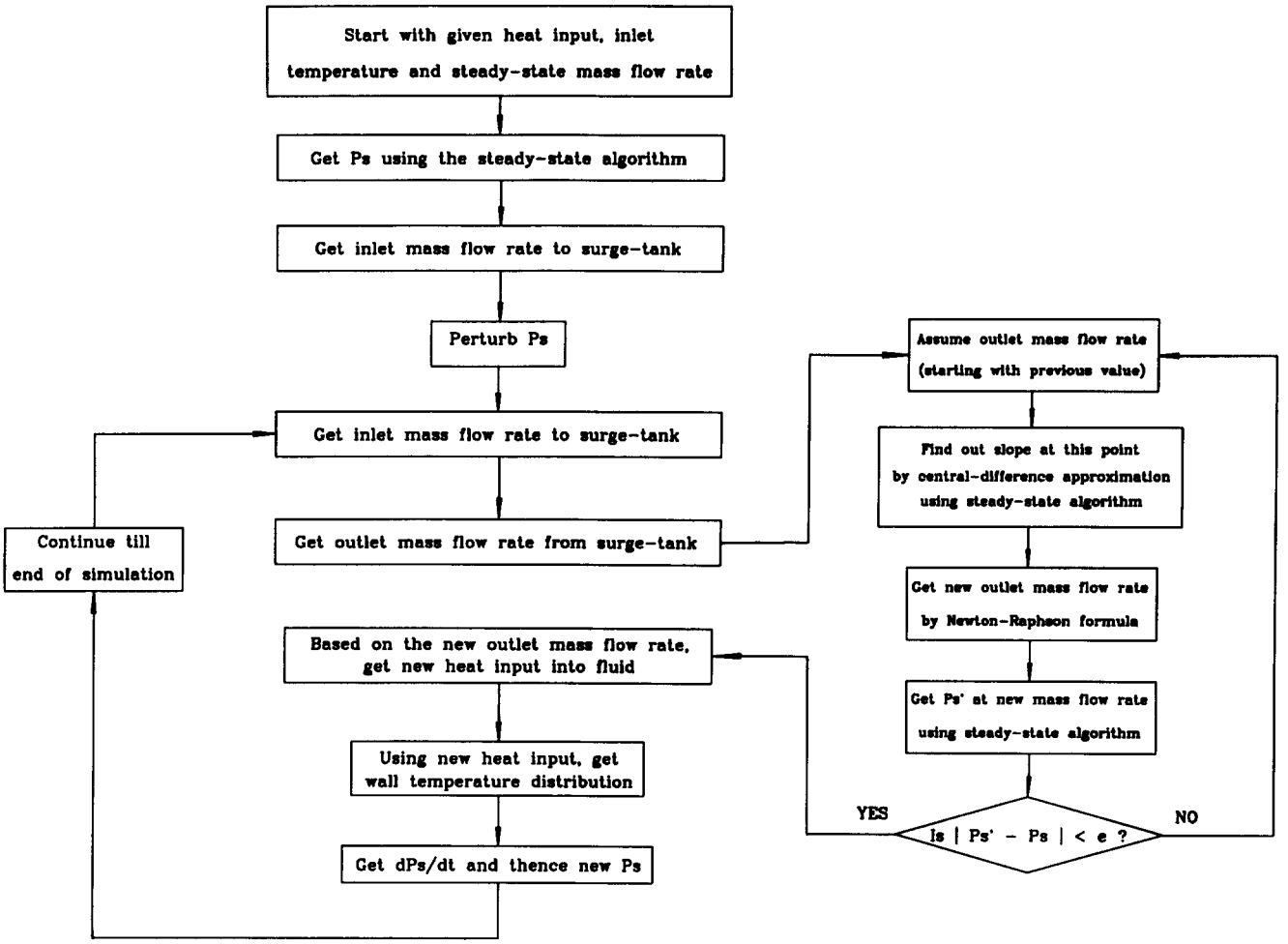

Figure 4 Flow-chart for the time-dependent solution algorithm

surge tank, and the changed inlet mass velocity for the surge tank is calculated. Calling the steady-state program again, the mass velocity and other flow parameters and properties along the system are computed, corresponding to the increased surge tank pressure. Since the pressure in the surge tank is increased, the flow rate through the heater decreases. The heat transfer coefficient and the heat input into the fluid also change. Next, the resultant surge tank pressure is calculated. This procedure is repeated in the successive time steps. The flowchart for this algorithm is presented in Figure 4.

In the successive time steps, the pressure difference between the surge tank and the system exit increases along the negative slope, until the top of one of the steady-state mass flow rate versus pressure-drop curves is reached, depending on the instantaneous heat input into the fluid. Then the calculation point leads from the top of the curve to the liquid region automatically. The flow rate through the heater increases. The surge tank pressure decreases with increasing flow rate through the heater, since the exit flow rate is larger than the inlet flow rate. The pressure in the surge tank decreases till the bottom of one of the steady-state mass flow rate versus pressure-drop curves. Then another flow excursion takes place from the liquid region to two-phase or vapor region. These limit cycles are then repeated.

Model for thermal oscillations. During the pressure-drop type oscillations, the mass flow rate, heat transfer coefficient, and heat input into the fluid keep changing. However, the heat generated in the heater wall by the electric current is constant. Therefore, when the limit cycle enters the liquid region, the wall temperature decreases as the liquid heat transfer coefficient is usually high; whereas when the limit cycle enters the vapor region, the wall temperature increases. Thus, the wall temperature keeps fluctuating during the limit cycle. These are termed as the thermal oscillations.

Governing equations

(a) Rate of heat transfer into the fluid

$$Q_I = \int_{A_h} \alpha(T_w - T_f)\, dA \tag{19}$$

The heat transfer coefficient α in Equation 19 is to be calculated under oscillating conditions, and is obtained from the following correlation[21]:

$$\mathrm{Nu} = 190 C_s \left(\frac{P}{P_c}\right)^{0.25} \left(\frac{q d_e}{h_{lv}\mu_l}\right)^{0.7} e^{-0.125x} \tag{20}$$

where $\mathrm{Nu} = \alpha d_e / k_l$, α is the local heat transfer coefficient, d_e is the effective diameter of the heater tube, k_l is the saturated liquid thermal conductivity, C_s is the dimensionless surface condition coefficient ($=1$ for bare tube), and q is the heat flux density.

(b) The heater wall temperature can be calculated from the

energy balance for the heater, yielding

$$\frac{d(T_w)}{dt} = \frac{(Q_o - Q_I)}{m_h c_h} \tag{21}$$

Method of solution

In the pressure-drop oscillation model, fluid parameters and properties are calculated along the system during the oscillations. The fluid temperature inside the heater at any node is known. The heat transfer coefficient is calculated using Equation 20. To start with, the heat input into the fluid is assumed. Then the heater wall temperature can be calculated. During the oscillations, the heat transfer coefficient and the heat input change, and the heater wall temperature changes accordingly.

The solutions of these equations, which are coupled with the hydraulics of the system, as described earlier, yield the thermal oscillations at any node of the heater.

Comparison of theoretical predictions with experimental results

Figures 5 through 7 show the theoretical predictions of the pressure-drop type and the thermal oscillations, along with the experimental results. The experimental cases are selected so

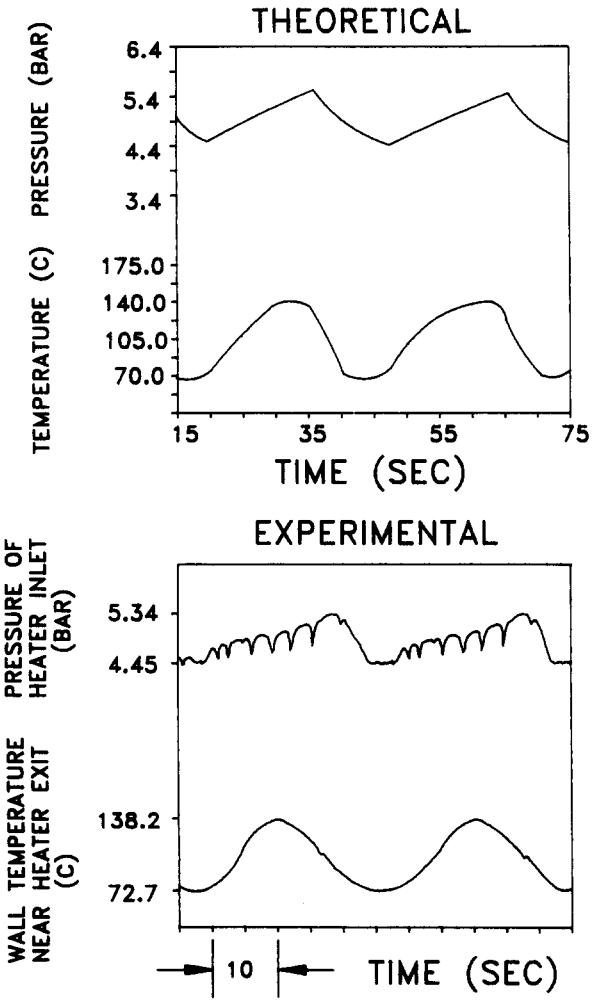

Figure 5 Comparison of theoretical predictions of pressure-drop type and thermal oscillations with experimental results. Heat input, 800 W, inlet fluid temperature, 23°C. Operating mass flow rate, 11.89 g/sec. Heater: coated nichrome, ID 7.5 mm, OD 9.5 mm

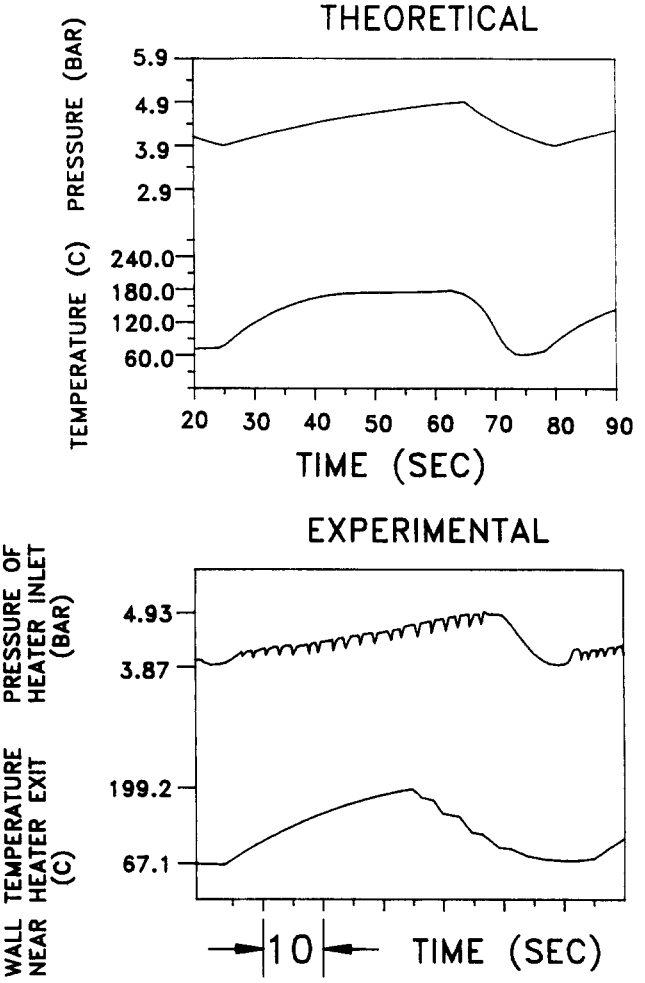

Figure 6 Comparison of theoretical predictions of pressure-drop type and thermal oscillations with experimental results. Heat input, 800 W, inlet fluid temperature, 0°C. Operating mass flow rate, 7.31 g/sec. Heater: coated nichrome, ID 7.5 mm, OD 9.5 mm

that at least two different cases of relevant parameters are represented, i.e., operating mass flow rate, heat input, inlet subcooling, and the heater surface condition. It can be seen that there is good agreement between the two. The periods, amplitudes, as well as the waveforms, of the oscillations are reasonably well predicted by the theory. Table 1 summarizes the comparison between the experimental and theoretical results.

The pressure-drop oscillations result through the interaction between the flow and the compressible volume in the surge-tank. Under the present experimental conditions, high frequency density-wave oscillations also occur, which are superimposed on the pressure-drop oscillations. The present model can predict the pressure-drop and thermal oscillations quite well. However, density-wave oscillations cannot be predicted by this model, because it does not take into account explicitly the propagation of continuity waves that generate those oscillations. Efforts are under way to extend the modeling methodology in order to predict the complete superimposed oscillations.

Conclusions

Experiments with various heat inputs have been conducted using nichrome tubes in a single channel upflow boiling system

Table 1 Comparison of experimental and theoretical results (Heater tube: nichrome, with ID 7.5 mm and OD 9.5 mm.)

Heater tube surface	Inlet temperature [°C]	Mass flow rate [g/sec]	Heat input [W]	Oscillation type and location	Experimental		Theoretical	
					Period [sec]	Ampli.	Period [sec]	Ampli.
Coated	23	7.31	800	Heater inlet pressure	50	0.96 [bar]	57	0.94 [bar]
				Heater exit temperature	50	99.8 [°C]	57	96.0 [°C]
Coated	23	11.89	800	Heater inlet pressure	28	0.89 [bar]	27	1.14 [bar]
				Heater exit temperature	28	65.6 [°C]	27	75.0 [°C]
Bare	23	7.31	600	Heater inlet pressure	25	0.50 [bar]	30	0.69 [bar]
				Heater exit temperature	25	49.2 [°C]	30	40.0 [°C]
Coated	0	7.31	800	Heater inlet pressure	60	1.06 [bar]	59	0.98 [bar]
				Heater exit temperature	60	132.1 [°C]	59	122.0 [°C]

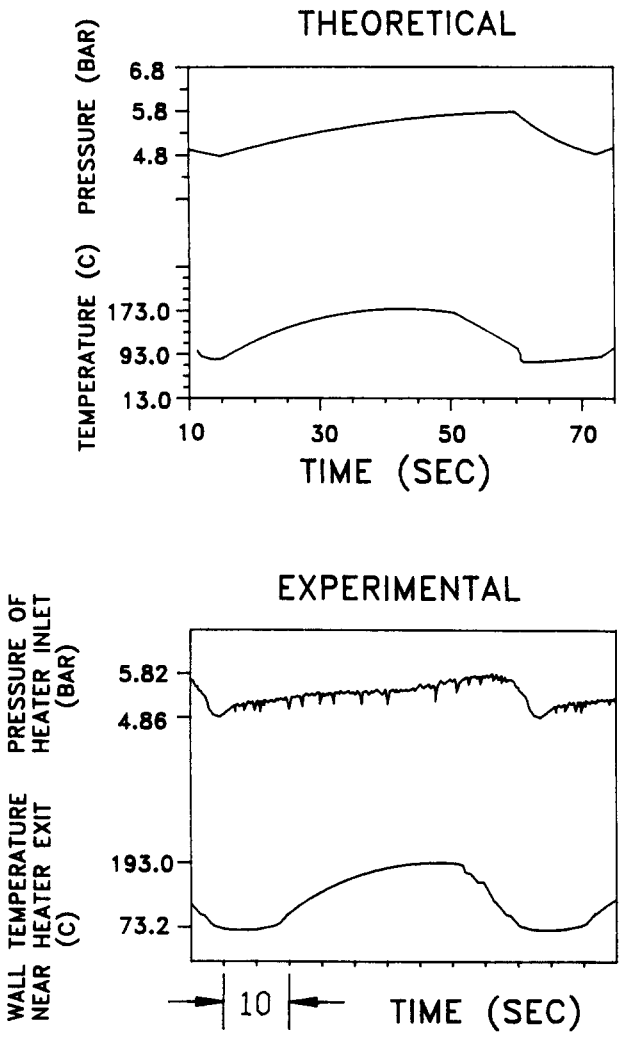

Figure 7 Comparison of theoretical predictions of pressure-drop type and thermal oscillations with experimental results. Heat input, 800 W, inlet fluid temperature, 23°C. Operating mass flow rate, 7.31 g/sec. Heater: coated nichrome, ID 7.5 mm, OD 9.5 mm

to study the pressure-drop type and thermal oscillations. Two tubes were used in the study: one coated with Linde High-flux coating and the other bare. Experiments have been performed at a constant inlet temperature for different heat inputs. In another series of experiments, the heat flux was kept constant and the inlet temperature varied. The drift flux formulation of two-phase flows has been developed to obtain the steady-state characteristics of the vertical channel system.

The following conclusions can be reached based on the experimental and theoretical studies:

- Both the pressure-drop type and thermal oscillations occur at all heat inputs. At a given inlet subcooling, the amplitudes and periods of the oscillations increase with increasing heat input rate.
- Both the pressure-drop type and thermal oscillations occur at all inlet subcoolings. At a given heat input rate, the amplitudes and periods of the oscillations increase with increasing inlet subcooling.
- Thermal oscillations accompany the pressure-drop type oscillations. Oscillations of pressure and temperature are in phase; but the maximum of pressure oscillations always lags as compared with the maximum of temperature oscillations.
- The periods and amplitudes of the oscillations increase with decreasing mass flow rate at the initial operating point on the negative slope.
- The steady-state characteristics and the oscillations predicted with the use of the drift flux model are in reasonably good agreement with experimental results.

Acknowledgment

This paper was revised and finalized during Professor Kakac's stay at the Lehrstuhl A für Thermodynamik, Technische Üniversität München, as a recipient of the US Senior Scientists Award from the Alexander von Humboldt Foundation.

The authors gratefully acknowledge the financial support of the National Science Foundation.

References

1 Ishii, M. Drift-flux model and derivation of kinematic constitutive laws. *Two-phase Flows and Heat Transfer* (Kakaç, S., Mayinger, F., and Veziroğlu, T. N., eds.). Hemisphere, New York, 1977

2 Yadigaroglu, G., and Lahey, R. T., Jr. On the various forms of conservation equations in two-phase flow. *Int. J. Multiphase Flow*, 1976, **2**, 477–484

3 Bourè, J. A. Mathematical modeling and two-phase constitutive equations. *European Two-phase Flow Group Meeting*, Haifa, Israel, 1975

4 Delhaye, J. M. Two-phase flow modeling. *Thermohydraulics of Two-phase Systems for Industrial Design and Nuclear Engineering* (Delhaye, J. M., Giot, M., and Riethmuller, M. L., eds.). Hemisphere, New York, 1981

5 Zuber, N., and Findlay, J. Average volumetric concentration in two-phase flow systems. *ASME J. Heat Transfer*, 1965, **87**, 453

6 Doğan, T., Kakaç, S., and Veziroğlu, T. N. Lumped parameter analysis of two-phase flow instabilities. *Proc. 7th Int. Heat Transfer Conf.*, Munchen, F.R.G., 1982, **5**, 213–218

7 Gürgenci, H., Veziroğlu, T. N., and Kakaç, S. Simplified descriptions of two-phase flow instabilities in a vertical boiling channel. *Int. J. Heat Mass Transfer*, 1982, **26**, 671–679

8 Lin, A. H., Zhang, X., Chen, X. J., Veziroğlu, T. N., and Kakaç, S. An analytical study of the pressure-drop type instabilities in a horizontal hairpin tube. *Int. J. Engg. Fluid Mech.*, 1988, **1**, No. 4

9 Menteş, A., Kakaç, S., Veziroğlu, T. N., and Zhang, H. Y. Effect of inlet subcooling on two-phase flow oscillations in a vertical boiling channel. *Warme-und Stoffubertragung*, 1989, **24**, 25–36

10 Kakaç, S., Veziroğlu, T. N., Padki, M. M., Fu, L. Q., and Chen, X. J. Investigation of thermal instabilities in a forced convection upward boiling system. *Int. J. Experimental Thermal and Fluid Science*, 1990, **3**, 191–201

11 Kakaç, S., Veziroğlu, T. N., Fu, L. Q., Chen, X. J., and Padki, M. M. Two-phase flow thermal instabilities in a vertical boiling channel. In *Fundamentals of Gas–Liquid Flows* (Michaelides, E. E., and Sharma, M. P., eds.). ASME, FED, **72**, 1988

12 Liu, H. T. Parametric study of two-phase flow instabilities in a forced-convective boiling upflow system. M.S. Thesis, University of Miami, Coral Gables, FL, 1989

13 Veziroğlu, T. N., and Kakaç, S. Two-phase flow instabilities. Final Report: NSF Project CME 79-20018, 1983

14 Park, G. C., Podowski, M., Becker, M., and Lahey, R. T., Jr. The modelling of density-wave oscillations in boiling water nuclear reactors. In *Advances in Two-phase Flows and Heat Transfer*. Martinus Nijhoff, The Netherlands, 1983

15 Yadigaroglu, G. Two-phase flow instabilities and propagation phenomena. In *Thermalhydraulics of Two-phase Systems for Industrial Design and Nuclear Engineering*. Hemisphere, New York, 1981

16 Delavarpour, K., and Akyuzlu, K. M. Numerical simulation of thermal hydrodynamic instabilities in two-phase flow systems using fully explicit finite-difference techniques. In *Multiphase Transport and Particulate Phenomena IV* (Veziroğlu, T. N., ed.). Hemisphere, New York, 1987, **III**, 631–640

17 Akyuzlu, K. M., and Morantine, M. C. Determination of regions with thermal-hydrodynamic stability at low mass flow rates in upward flow systems. In *Fundamental Aspects of Gas–Liquid Flows* (Michaelides, ed.). American Society of Mechanical Engineers, New York, FED, **29**, 1985, 173–179

18 Clausse, A., Delmastro, D., and Lahey, R. T., Jr. The analysis of chaotic instabilities in natural circulation boiling systems. Eurotherm Seminar, 16, Natural Circulation in Industrial Applications, Pisa, October 11–12, 1990

19 Rizwan-Uddin, and Dorning, J. J. Some nonlinear dynamics of a heated channel. *Nuc. Eng. Des.*, **93**, 1, 1986

20 Lahey, R. T., Jr., and Moody, F. J. The thermal-hydraulics of a boiling water nuclear reactor. Chapter 7, ANS Monograph, 1977

21 Lin, Z. H., Veziroğlu, T. N., Kakaç, S., Gürgenci, H., and Mentes, A. Heat transfer in oscillating two-phase flow and effect of heater surface conditions. *Proc. 7th Int. Heat Transfer Conference*, München, Federal Republic of Germany, **5**, 331–336, 1982